Tail-free self-accelerating solitons and vortices

Jieli Qin,[1,2] Zhaoxin Liang,[3] Boris A. Malomed,[4] and Guangjiong Dong[1]

[1]*State Key Laboratory of Precision Spectroscopy, East China Normal University, 3663 North Zhongshan Road, Shanghai, China and Collaborative Innovation Center of Extreme Optics, Shanxi University, Taiyuan, Shanxi 030006, China*

[2]*School of Physics and Electronics Engineering, Guangzhou University, 230 Guangzhou University City Outer Ring Road, Guangzhou, Guangdong 510006, China*

[3]*Department of Physics, Zhejiang Normal University, Jinhua, Zhejiang 321004, China*

[4]*Department of Physical Electronics, School of Electrical Engineering, Faculty of Engineering, and Center for Light-Matter Interaction, Tel Aviv University, Ramat Aviv 69978, Israel*

(Received 10 March 2018; published 7 February 2019)

Self-accelerating waves in conservative systems, which usually feature slowly decaying tails, such as Airy waves, have drawn great interest in studies of quantum and classical wave dynamics. They typically appear in linear media, while nonlinearities tend to deform and eventually destroy them. We demonstrate, by means of analytical and numerical methods, the existence of robust one- and two-dimensional (1D and 2D) self-accelerating tailless solitons and solitary vortices in a model of two-component Bose-Einstein condensates, dressed by a microwave (MW) field, whose magnetic component mediates long-range interaction between the matter-wave constituents, with the feedback of the matter waves on the MW field taken into account. In particular, self-accelerating 2D solitons may move along a curved trajectory in the coordinate plane. The system may also include the spin-orbit coupling between the components, leading to similar results for the self-acceleration. The effect persists if the contact cubic nonlinearity is included. A similar mechanism may generate 1D and 2D self-accelerating solitons in optical media with thermal nonlinearity.

DOI: 10.1103/PhysRevA.99.023610

I. INTRODUCTION

Self-accelerating Airy waves were predicted in the context of quantum mechanics [1]. Then this concept was transferred to optics [2], plasmonics [3], acoustics [4], gas discharge [5], and hydrodynamics [6], using the similarity of the linear Schrödinger equation to the paraxial wave-propagation equation in classical physics. These wave modes offer applications to plasma guiding [7], signal transmission [8,9], laser-beam filamentation [10], optical micromanipulation [11–16], generation of "light bullets" [17–20], and so on [21–23].

Quantum self-accelerating waves have been experimentally demonstrated in electron optics [24]. Self-accelerating Dirac waves have also been predicted in relativistic quantum mechanics [25]. Coherent Bose-Einstein condensates (BECs) may be appropriate for the realization of the self-acceleration in matter waves. The latter effect has not yet been demonstrated experimentally, although it has been elaborated theoretically, assuming the use of laser beams to imprint appropriate phase modulation onto the BEC [26] or the use of a trapping potential moving with acceleration [27].

Ideal Airy waves with slowly decaying oscillatory tails carry an infinite norm, therefore truncated Airy waves with a finite norm were used in the theory and experiments [2,28]; however, the truncation causes gradual decay of the self-accelerating wave packets. Furthermore, the study of the evolution of the Airy waves, which are eigenmodes of the linear propagation, in various nonlinear media [28–42] shows that the nonlinearity causes deformation and often destruction of the self-accelerating waves. Another type of self-accelerating solitary-wave pairs was predicted [43] and demonstrated experimentally [44] in nonlinear photonic crystals with opposite signs of the dispersion (effective mass) for the paired modes.

The above-mentioned settings were implemented neglecting dissipation in the medium. On the other hand, robust optical tail-free self-accelerating pulses have been predicted and experimentally demonstrated under the action of various nonconservative effects, such as the sliding-frequency filtering [45], ionization of the dielectric medium [46], diffusion in photorefractive crystals [47], and intrapulse stimulated Raman scattering [48]. In the latter case, the number of photons (integral norm of the pulse) is conserved, but the Raman effect breaks the conservation of the momentum and Hamiltonian.

The present work shows that the long-range nonlinear interaction between constituents of a binary BEC, mediated by a microwave (MW) field (this interaction was elaborated in Refs. [49,50]), supports spatially symmetric tail-free self-accelerating hybrid solitons, both one- and two-dimensional (1D and 2D) ones, built of matter-wave and MW components (in that sense, they resemble exciton-polariton solitons, which are also matter-field hybrids [51], although the present model is a strictly conservative one, while exciton-polaritons states exist in dissipative semiconductor cavities and therefore they should be supported by pump fields). It is relevant to stress that both the self-trapping and self-acceleration are induced by the same interaction, while in previously studied nonlinear systems the acceleration was driven by terms such as the induced-Raman-scattering one, while the self-trapping was provided by the Kerr nonlinearity. Further, we demonstrate that the self-acceleration mechanism works equally well in

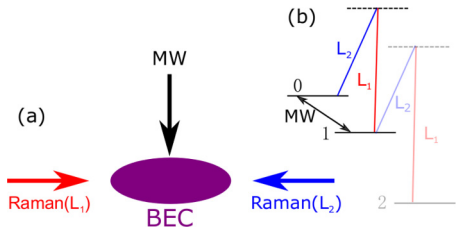

FIG. 1. (a) Counterpropagating Raman beams L_1 and L_2 generate the spin-orbit-coupled two-component BEC, as shown in Ref. [52]. (b) The microwave field couples states 0 and 1 by an effective long-range interaction [see Eqs. (1) and (4)].

the presence of the spin-orbit coupling (SOC) between the two components of the BEC wave function, as well as in the presence of the usual nonlinear contact interactions. In addition to the results for the matter-wave solitons, it is demonstrated that similar self-accelerating optical solitons can be produced in conservative optical media with strongly nonlocal nonlinearity.

The rest of the paper is organized as follows. The 1D model is formulated in Sec. II, which includes the linear SOC effect in the two-component BEC. Both analytical and numerical systematic results for the self-acceleration for 1D solitons are reported in Sec. III. The 2D extension of the model is presented in Sec. IV, where emphasis is put on the stable self-acceleration of vortices. This section also includes a brief consideration of a nonlocal optical system which may be represented by a similar model, thus predicting similar results for 1D and 2D self-accelerating spatial optical solitons. The paper is summarized in Sec. V.

II. THE ONE-DIMENSIONAL SYSTEM

Because some essential results reported below are obtained for the binary BEC including the SOC effect, it is relevant to outline its implementation in the relevant setting. It may be realized using the scheme shown in Fig. 1 [52]: counterpropagating Raman laser beams L_1 and L_2 drive the atomic gas, adiabatically eliminating level 2 and creating the SOC system with pseudospin 1/2, whose components represent atoms in states 0 and 1. The emulation of various aspects of gauge physics in ultracold gases by means of SOC has drawn a great deal of interest [53–75]. In particular, SOC solitons have been predicted in 1D [76,77], 2D [78–80], and 3D [81] geometries (see also a review in [82]). However, SOC breaks the Galilean invariance, which makes the creation of moving solitons a nontrivial issue [77–79]. It was found that 2D solitons in the system with SOC of the Rashba type feature mobility only in one direction, up to a critical value of the velocity, beyond which delocalization occurs [78]. Self-accelerating solitons have not been found in previous works dealing with SOC models.

We consider here the pseudospinor BEC with two components coupled by the interaction mediated by the magnetic component of the MW field, as schematically shown in Fig. 1 [49]. It has been found that the interaction gives rise to quiescent hybrid MW–matter-wave solitons in one dimension [49], as well as to giant solitary vortices in two dimensions, which are stable at least up to topological charge $S = 5$ [50]. The solitons persist in the presence of additional contact interactions of either sign, corresponding to self- and cross-attraction or repulsion of the pseudospinor's components.

In the 1D setting, components of the pseudospinor wave function $\Psi \equiv \binom{\Psi_\downarrow}{\Psi_\uparrow}$, which correspond to states 0 and 1 in Fig. 1, coupled by the MW magnetic-field potential H, obey coupled Gross-Pitaevskii equations (GPEs), which may or may not include the SOC terms with strength K, represented by the first spatial derivatives, which are combined with the Rabi-coupling frequency Ω:

$$i\partial_t \begin{pmatrix} \Psi_\downarrow \\ \Psi_\uparrow \end{pmatrix} = \left[-\frac{1}{2}\partial_x^2 + U(x) + \begin{pmatrix} iK\partial_x & \Omega - H \\ \Omega - H^* & -iK\partial_x \end{pmatrix} - \begin{pmatrix} \beta_1|\Psi_\downarrow|^2 + \beta_2|\Psi_\uparrow|^2 & 0 \\ 0 & \beta_1|\Psi_\uparrow|^2 + \beta_2|\Psi_\downarrow|^2 \end{pmatrix} \right] \begin{pmatrix} \Psi_\downarrow \\ \Psi_\uparrow \end{pmatrix}. \tag{1}$$

Real coefficients β_1 and β_2 represent here, severally, the self- and cross-component contact interactions, $\beta_{1,2}>0$ (<0) corresponding, respectively, to the attractive (repulsive) sign of the interactions. The wave function is subject to the normalization

$$\int_{-\infty}^{+\infty} \Psi^\dagger \Psi \, dx = 1. \tag{2}$$

The feedback of the matter-wave components on the MW potential (a specific manifestation of the general *local field effect* [83]) is accounted for by the Poisson equation [49]

$$\partial_x^2 H = -\gamma \Psi_\downarrow^* \Psi_\uparrow, \tag{3}$$

whose solution can be written with the help of the 1D Green's function

$$H(x,t) = -\frac{\gamma}{2} \int_{-\infty}^{+\infty} |x - x'| \Psi_\downarrow^*(x',t) \Psi_\uparrow(x',t) dx'. \tag{4}$$

Note that the asymptotic form of the potential, produced by Eq. (4) at $|x| \to \infty$, is a linear function of the coordinate, which is a commonly known property of solutions to the 1D Poisson equation with a localized source of the field:

$$H(x) \approx -\chi |x|, \quad \chi \equiv \frac{\gamma}{2} \int_{-\infty}^{+\infty} \psi_\downarrow^*(x) \psi_\uparrow(x) dx. \tag{5}$$

In the presence of SOC [Eq. (1)], the position, energy, and time are scaled, respectively, by the inverse SOC wave number k^{-1}, recoil energy $E_R \equiv \hbar^2 k^2/2m$, and $\hbar/E_R$ so that $K \equiv 1$ is fixed in Eq. (1), unless we consider the system without SOC, by setting $K = 0$. Further, $U(x)$ in Eq. (1) is a trapping potential (actually, we aim to consider free-space solitons, with $U = 0$) and

$$\gamma \equiv Nm\varepsilon_0 \mu_0^2 \omega_{\rm MW}^2 M^2/\hbar^2 A k^3 \tag{6}$$

is the effective strength of the MW-mediated long-range interaction, with ε_0 and μ_0 the vacuum permittivity and permeability, respectively, N the number of atoms, m the atomic mass, $\omega_{\rm MW}$ the MW frequency, M the atomic magnetic moment, and A the confinement area in the transverse plane. Considering, for instance, BECs of ^{87}Rb atoms, transversely confined in an area $\sim 1\ \mu{\rm m}^2$, coupled to the MW with a wave-

length of ∼1 mm, and the action of SOC with wavenumber $k \sim 1\ \mu\text{m}^{-1}$, Eq. (6) yields $\gamma \sim 10^{-9}N$. Thus, for BECs of 10^7 atoms (actually, condensates made of up to 10^8 atoms are available, according to current experimental results [84]), one obtains $\gamma \sim 10^{-2}$. Following this estimate, we set $\gamma = 0.02$ in numerical simulations below. Furthermore, by using even tighter transverse confinement to reduce the transverse-localization area A, the necessary number of atoms can be made essentially smaller than 10^7, which is used here as the estimate.

III. SELF-ACCELERATING ONE-DIMENSIONAL SOLITONS

First, it is necessary to produce stationary solitons with real chemical potential μ, in the form

$$\Psi(x,t) = \begin{pmatrix} \psi_\downarrow(x) \\ \psi_\uparrow(x) \end{pmatrix} e^{-i\mu t}, \tag{7}$$

with the pseudo-spin-up and -down components of the complex spinor wave function $\psi_{\uparrow,\downarrow}(x)$ obeying the stationary free-space version of Eq. (1), with $U(x) = 0$:

$$\mu \begin{pmatrix} \psi_\downarrow \\ \psi_\uparrow \end{pmatrix} = \left[-\frac{1}{2}\partial_x^2 + \begin{pmatrix} iK\partial_x & \Omega - H \\ \Omega - H^* & -iK\partial_x \end{pmatrix} - \begin{pmatrix} \beta_1|\psi_\downarrow|^2 + \beta_2|\psi_\uparrow|^2 & 0 \\ 0 & \beta_1|\psi_\uparrow|^2 + \beta_2|\psi_\downarrow|^2 \end{pmatrix} \right] \begin{pmatrix} \psi_\downarrow \\ \psi_\uparrow \end{pmatrix}. \tag{8}$$

Actually, it is more convenient to produce the stationary wave function not through Eq. (8), but rather by solving Eqs. (1) and (4) by dint of the imaginary-time-integration method. The simulations were carried out in the domain $|x| \leqslant 80$, or in a smaller one, if it was sufficient for a particular situation, with zero boundary conditions at the edges of the domain. As a result, three distinct species of the 1D solitons have been identified, viz., those of the regular, stripe, and plane-wave types (solitons of the latter type are carried by the plane-wave phase, discussed below). In the most fundamental case, when the contact interactions are absent, i.e., $\beta_{1,2} = 0$ in Eq. (1), and solitons may only be supported by the MW-mediated interaction, typical examples of the three species are displayed, respectively, in Figs. 2(a1) ($\Omega = 1.5$), 2(b1) ($\Omega = 0.7$), and 2(c1) ($\Omega = 0.7$) for $\gamma = 0.02$, along with the respective profiles in the momentum space, in Figs. 2(a2), 2(b2), and 2(c2). In particular, the stripe and plane-wave-type solitons coexist at the same values of parameters, being almost mutually degenerate under the normalization condition (2), with chemical potentials $\mu = -0.7300$ and -0.7298, respectively. A distinctive peculiarity of the soliton of the plane-wave type is asymmetry between its components.

The soliton of the regular type, presented in Figs. 2(a1) and 2(a2) for $\Omega^2 > 1$, resembles those in the usual 1D SOC model (which does not include the MW-mediated coupling between the components) [85], with zero carrier wave number $p_x = 0$, while at $\Omega^2 < 1$ the formal linearization of Eq. (1) for tails of solitons [which implies setting $H = 0$, according to Eq. (4)] demonstrates that they may develop oscillations with wave numbers $p_x = \pm\sqrt{\sqrt{\mu^2 - \Omega^2} + 1 - |\mu|}$ (the solitons exist at $\mu < -1$). Solitons carried by p_x with the single sign are categorized as modes of the plane-wave type, while the superposition of the two wave numbers with opposite signs gives rise to stripe solitons [75]. However, the MW potential H, dressing the condensate, completely changes the asymptotic shape (tails) of localized modes at large $|x|$, where, taking Eq. (5) into consideration, Eq. (8) reduces to

$$\mu\psi = \begin{pmatrix} -\frac{1}{2}\partial_x^2 + iK\partial_x & \Omega + \chi|x| \\ \Omega + \chi^*|x| & -\frac{1}{2}\partial_x^2 - iK\partial_x \end{pmatrix} \psi, \tag{9}$$

with χ defined as per Eq. (5).

The presence of the effective linear potential $\sim|x|$ in the asymptotic equation (9) suggests to approximate solutions by Airy functions [1]. Accordingly, the variational approximation (VA) for solutions to Eq. (8) may be based on the ansatz

$$\psi^{(\text{VA})} = \left[\cos\alpha \begin{pmatrix} \cos\theta \\ \sin\theta \end{pmatrix} e^{-ip_0 x} - \sin\alpha \begin{pmatrix} \sin\theta \\ \cos\theta \end{pmatrix} e^{+ip_0 x} \right] \phi(x), \tag{10}$$

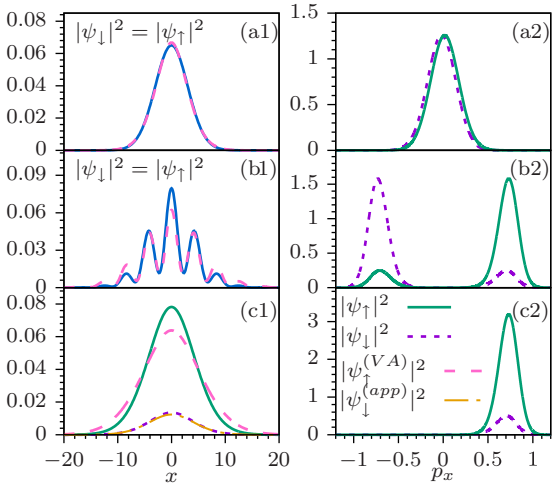

FIG. 2. Typical density profiles in the (a1), (b1), and (c1) coordinate space and (a2), (b2), and (c2) momentum space (produced by the Fourier transform of the coordinate profile) of (a) a regular (single-peak) soliton, (b) a stripe soliton, and (c) a soliton of the plane-wave type, so called because it is carried by the plane-wave phase, for the pseudo-spin-up (solid lines) and pseudo-spin-down (short-dashed lines) components. These solutions to Eq. (1), with $K \equiv 1$ and $\beta_{1,2} = 0$, were obtained, by means of the imaginary-time integration, at $\Omega = 1.5$, $\Omega = 0.7$, and $\Omega = 0.7$, with the respective chemical potentials $\mu = -1.4779$, -0.7300, and -0.7298. The wave functions predicted by the VA (long-dashed lines), $\psi_\uparrow^{(\text{VA})}(x)$, based on the ansatz defined by Eqs. (10) and (11), with VA-predicted chemical potentials -1.4781, -0.7262, and -0.7260, respectively, are plotted too for comparison with the numerical results in the coordinate space. In (c1), the approximate wave function $\psi_\downarrow^{(\text{app})}$ for the pseudo-spin-down component, produced by the separately developed analytical approximation (13), is plotted by the yellow dash-dotted line, which overlaps with its numerical counterpart.

where the shape function is chosen as

$$\phi(x) = \psi_0 \mathrm{Ai}(|x|/\sigma + \xi_0), \tag{11}$$

where $\xi_0 \approx -1.019$ is the first local maximum of the Airy function $\mathrm{Ai}(\xi)$ and hence $x = 0$ is the center of the adopted profile. The variational parameters are α, θ, p_0, and σ, while ψ_0 is a normalization constant. In contrast, in the usual 1D SOC model, which does not include the MW field, $\phi(x)$ is approximated by a sech or Gaussian ansatz [75]. At $\alpha = 0$ or $\pi/2$, the ansatz (10) reduces to an envelope multiplying the plane wave, while at $\alpha = \pi/4$, depending on Ω, the ansatz may represent either a stripe soliton, if the wavelength $2\pi/p_0$ is small in comparison with the envelope's width, or a regular single-peak soliton otherwise. The values of the variational parameters are numerically determined by minimizing the system's energy

$$E = \int_{-\infty}^{+\infty} dx\, \psi^\dagger \left[-\frac{1}{2}\frac{d^2}{dx^2} + \begin{pmatrix} iK\partial_x & \Omega \\ \Omega & -iK\partial_x \end{pmatrix} \right] \psi + \frac{\gamma}{4} \iint dx\, dx' |x - x'| \times [\psi_\downarrow^*(x)\psi_\uparrow(x)\psi_\downarrow^*(x')\psi_\uparrow(x') + \text{c.c.}]. \tag{12}$$

In Eq. (12), the contact interactions are again disregarded, setting $\beta_{1,2} = 0$ in Eq. (1), aiming to address the fundamental setting, with the two components of the pseudospinor wave function interacting solely via the MW magnetic field. The VA-predicted soliton profiles are displayed in Fig. 2 along with their numerically found counterparts, demonstrating that the VA is reasonably accurate, providing in particular an accurate approximation for the regular solitons.

The MW-mediated long-range interaction, which is the underlying ingredient of the present system, determines not only the shape of the solitons, but also their dynamics, as shown by systematic simulations of Eq. (1). It was found that the addition of small random perturbations to the regular and stripe solitons does not produce any conspicuous effect (which implies that they are completely stable modes in the quiescent state), while perturbed solitons of the plane-wave type start self-accelerated motion, keeping their integrity, as shown in Fig. 3 for the system without the contact interactions ($\beta_{1,2} = 0$).

Stable self-accelerating solitons persist in the presence of the contact nonlinearity with the repulsive sign, as shown in Fig. 4, as well as under the action of relatively weak local attraction (see Fig. 5). Strong attraction may change the situation, as it tends to transform the solitons considered here, characterized by the ansatz based on Eqs. (10) and (11), into usual sech-shaped solitons, for which the interaction with the MW field becomes negligible. Naturally, the strong self-repulsion makes the moving soliton much broader, as can be seen in Fig. 4. As concerns the gradual decrease of the acceleration, observed in Fig. 4, starting from $t \simeq 4500$, and in Fig. 5, starting from $t \simeq 7000$, detailed consideration of the numerical data demonstrates that this effect is explained by a brake force, which is applied to the soliton by radiation emitted by it at the initial stage of the evolution and eventually reflected from the edge of the integration domain.

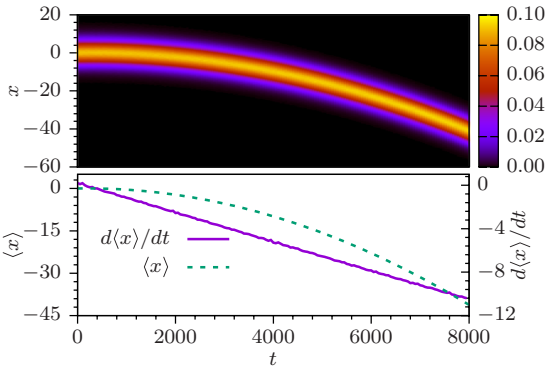

FIG. 3. Shown on top is the evolution of the same plane-wave-type soliton as in Fig. 2 (i.e., in the absence of the contact interactions, $\beta_{1,2} = 0$), initiated by the addition of a small random perturbation to it. In this figure and similar ones displayed below, the evolution is displayed by means of the map of the total density of both matter-wave components in the (x, t) plane. Shown on the bottom is the soliton's average position $\langle x(t)\rangle \equiv \int_{-\infty}^{+\infty} \Psi^\dagger(x)\Psi(x)x\, dx$ and velocity $d\langle x(t)\rangle/dt$ as functions of time. The time dependence of the velocity helps to evaluate the soliton's acceleration (weak jitter in $d\langle x\rangle/dt$ is caused by the randomness of the initial perturbation).

These results suggest the existence of a family of stable self-accelerating solitons of the plane-wave type, including the quiescent and moving solitons displayed in Figs. 2(c1) and 2(c2) and Fig. 3, respectively, the acceleration being an internal parameter of the family. In the system dominated by the SOC terms, the family can be constructed in an analytical form. To this end, we look for the corresponding solution to Eq. (1) as $\Psi_{\uparrow\downarrow}(x, t) = \exp(ip_0x - i\mu t)\phi_{\uparrow\downarrow}(x, t)$, with slowly varying amplitudes $\phi_{\uparrow\downarrow}(x, t)$, carrier momentum p_0, and chemical potential μ. Using Eq. (1), the small component $\phi_\downarrow$ [see Fig. 2(c1)] is eliminated in favor of the larger one

$$\phi_\downarrow(x) \approx C(H^* - \Omega)\phi_\uparrow(x), \tag{13}$$

with $C \equiv (p_0 - \mu + p_0^2/2)^{-1}$ [recall that we set $K \equiv 1$ in Eq. (1), if the SOC terms are present]. This approximation for $\phi_\downarrow(x)$ is plotted in Fig. 2(c1) by means of the yellow dash-dotted curve, showing very good agreement with its numerically found counterpart. Further, substituting Eq. (13) in the remaining equation for $\phi_\uparrow$ in system (1) leads, in the

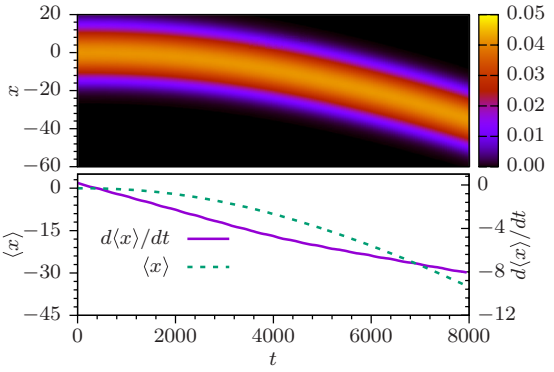

FIG. 4. Same as in Fig. 3, but in the presence of the self-repulsive contact interactions in Eq. (1) with $\beta_1 = -5.0$ and $\beta_2 = 0$.

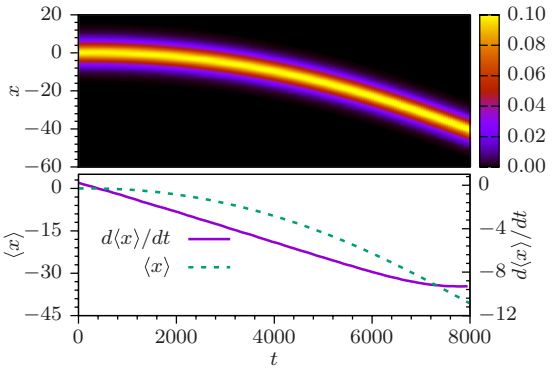

FIG. 5. Same as in Fig. 3, but in the presence of the self-attractive contact interactions in Eq. (1) with $\beta_1 = 0.3$ and $\beta_2 = 0$.

first approximation,[1] to a single GPE, in which the term $CH^*\phi_\uparrow$ from Eq. (13) couples the wave function $\phi_\uparrow$ to the potential H:

$$i\partial_t\phi_\uparrow = \left[-\tfrac{1}{2}\partial_x^2 - i(p_0-1)\partial_x + 2C\Omega H - \beta_1|\phi_\uparrow|^2\right]\phi_\uparrow. \tag{14}$$

Further, the substitution of the relation (13) in Eq. (3) leads to the Poisson equation, which gives rise to real MW potential H [unlike the complex field, produced by Eqs. (3) and (4) in the general case]:

$$\partial_x^2 H = C\gamma\Omega|\phi_\uparrow|^2. \tag{15}$$

Then the existence of self-accelerating solitons is explained by the fact that Eqs. (14) and (15) are invariant with respect to an *exact transformation* from the laboratory reference frame to one moving at an arbitrary constant acceleration a (while the usual GPE, as well as nonlinearly coupled GPE systems, is not invariant with respect to this transformation [86,87]):

$$\phi_\uparrow = \phi'_\uparrow(x',t)\exp\left[i\left(axt + \frac{1-p_0}{2}Ct^2 - \frac{a^2t^3}{6}\right)\right],$$
$$x' = x - (a/2)t^2, \quad H' = H + (2C\Omega)^{-1}ax. \tag{16}$$

Thus, any quiescent soliton produced by Eqs. (14) and (15) generates a family of solitons moving with arbitrary acceleration a, which is indeed the intrinsic parameter of the family, as conjectured above. In particular, the term $(2C\Omega)^{-1}ax$, added to the MW potential by the transformation, naturally breaks the symmetry of the linear in x asymptotic field (5) with respect to $x > 0$ and $x < 0$.

Note that, when $p_0 = 1$ [i.e., the SOC term vanishes in Eq. (14)], the transformation (16) remain valid and Eqs. (14) and (15) are tantamount to the model introduced in Ref. [49] without SOC (however, moving solitons were not considered in that work). Thus, the existence of the family of robust self-accelerating solitons does not depend on the presence of the SOC terms in Eq. (1) and it is not broken either by the inclusion of the contact-interaction term with the coefficient $-\beta_1$. The invariance with respect to the self-accelerating transformation cannot be produced in an exact form for the full system of equations (1) and (3), but its ability to maintain the self-acceleration is clearly demonstrated by numerical results (in particular, by Figs. 3–5).

The GPE system may also be reduced to a single equation in the case opposite to that considered above, namely, if the Rabi coupling dominates over SOC in Eq. (1), i.e., Ω is a large parameter. In this case, the substitution of

$$\Psi_\uparrow(x,t) = \exp[ix + (1/2-\mu_0)it]\Phi_\uparrow(x,t),$$
$$\Psi_\downarrow(x,t) = \exp[-ix + (1/2-\mu_0)it]\Phi_\downarrow(x,t), \tag{17}$$

with $\mu_0 = \pm\Omega$ and slowly varying amplitudes $\Phi_{\uparrow\downarrow}(x,t)$, yields a relation between them,

$$\Phi_\downarrow \approx \mu_0^{-1}(\Omega - H^*)e^{2ix}\Phi_\uparrow. \tag{18}$$

In contrast to the above case, when the component $\phi_\downarrow$ is small in comparison with $\phi_\uparrow$, as per Eq. (13), Eq. (18) implies that the absolute values of the two components are nearly equal. Eventually, the substitution of the expressions (17) and (18) in Eqs. (23) and (3) leads to the equations, which differ from Eq. (14) with $p_0 = 1$ (without the SOC term) and Eq. (15) only by the notation for coefficients,

$$i\partial_t\Phi_\uparrow = \left[-\left(\tfrac{1}{2}\right)\partial_x^2 \mp 2H(x) - (\beta_1+\beta_2)|\Phi_\uparrow|^2\right]\Phi_1,$$
$$\partial_x^2 H = \mp\gamma|\Phi_\uparrow(x')|^2,$$

i.e., the single GPE limit is a *universal* one, being equally relevant in the cases of strongly unequal and nearly equal components of the pseudospinor wave function.

IV. TWO-DIMENSIONAL SYSTEMS

A. The pseudospinor condensate coupled by the microwave field

In the 2D setting, Eqs. (1) and (3) are replaced by equations which combine the 2D version of SOC [78–80] and the interaction of the pseudospinor wave function with the MW field in two dimensions [50]:

$$i\partial_t\begin{pmatrix}\Psi_\downarrow\\ \Psi_\uparrow\end{pmatrix} = \left[-\frac{1}{2}\left(\partial_x^2+\partial_y^2\right) + \begin{pmatrix} iK\partial_x & K\partial_y + \Omega - H \\ -K\partial_y + \Omega - H^* & -iK\partial_x\end{pmatrix}\right]\begin{pmatrix}\Psi_\downarrow\\ \Psi_\uparrow\end{pmatrix}$$
$$-\begin{pmatrix}\beta_1|\Psi_\downarrow|^2 + \beta_2|\Psi_\uparrow|^2 & 0\\ 0 & \beta_1|\Psi_\uparrow|^2 + \beta_1|\Psi_\downarrow|^2\end{pmatrix}\begin{pmatrix}\Psi_\downarrow\\ \Psi_\uparrow\end{pmatrix}, \tag{19}$$

$$\left(\partial_x^2+\partial_y^2\right)H = -\gamma\Psi_\downarrow^*\Psi_\uparrow. \tag{20}$$

[1] A shift of the chemical potential $p_0^2/2 - p_0 - C\Omega^2 - \mu$ and a term $\sim|H|^2$ are neglected here, as they are small in comparison with the term kept in Eq. (14).

To provide straightforward insight into the dynamics of the 2D system, we again resort to the limit case of the strong Rabi coupling between the two components in Eq. (20), which dominates over SOC. Then two components of the pseudospinor may be reduced to one [cf. Eq. (18)] and the system of Eqs. (19) and (20) amounts to the single-component GPE coupled to the 2D Poisson equation, i.e., as a matter of fact, the 2D extension of Eqs. (14) and (15),

$$i\partial_t \Phi_\uparrow = -\tfrac{1}{2}\left(\partial_x^2 + \partial_y^2\right)\Phi_\uparrow \mp 2\,\mathrm{Re}(H)\Phi_\uparrow - (\beta_1+\beta_2)|\Phi_\uparrow|^2\Phi_\uparrow, \tag{21}$$

$$\left(\partial_x^2 + \partial_y^2\right)H = \mp\gamma|\Phi_\uparrow|^2. \tag{22}$$

A straightforward but crucially important fact is that, similar to what was found above for the 1D system [see Eq. (16)], Eqs. (21) and (22) are invariant with respect to the transformation to the reference frame which moves in the 2D space with arbitrary initial velocities V_x and V_y and arbitrary constant accelerations a_x and a_y:

$$\begin{aligned} &x' = x - V_x t - \tfrac{1}{2}a_x t^2, \quad y' = y - V_y t - \tfrac{1}{2}a_y t^2, \\ &H = H' \pm (a_x x + a_y y)/2, \\ &\Phi_\uparrow = \Phi'_\uparrow(x', y', t)\exp\{i[a_x t + V_x)x + (a_y t + V_y)y - \phi(t)]\}, \\ &\phi(t) = \frac{(a_x t + V_x)^3 - V_x^3}{6a_x} + \frac{(a_y t + V_x t)^3 - V_y^3}{6a_y}. \end{aligned} \tag{23}$$

Accordingly, the coordinates (x_c, y_c) of the center of the stable 2D soliton (which may carry embedded vorticity [50]) move as $x_c = V_x t + \frac{1}{2}a_x t^2$ and $y_c = V_y t + \frac{1}{2}a_y t^2$, which may be a curvilinear trajectory in the 2D plane: At small t, it is close to a straight line with slope $x/y = V_x/V_y$, while at $t \to \infty$ it becomes asymptotically close to a line with $x/y = a_x/a_y$. In particular, in the case of $a_x = V_y = 0$ the trajectory is a parabola: $y_c = (a_y/2V_x^2)x_c^2$.

Note that the solution of the 2D Poisson equation (22) has the standard logarithmic asymptotic form far from the region where the source of the field is located:

$$H \approx \mp\frac{\gamma}{2\pi}\left(\iint |\Phi_\uparrow(x, y)|^2 dx\, dy\right)\ln r. \tag{24}$$

The difference in the field component of the self-accelerating 2D solitons from that of their quiescent counterparts is more essential than in the 1D case, as the potential terms linear in x and y [see Eq. (23)] are qualitatively different from the logarithmic term in Eq. (24).

The predictions are corroborated, in Figs. 6 and 7, by numerical solutions of Eqs. (21) and (22) (in the absence and presence of the contact interaction, severally) for stable 2D solitons with embedded vorticity $S = 1$ (vortex rings), which move at a constant acceleration in the x direction, in exact agreement with Eq. (23). A remarkable fact is that, in the case shown in Fig. 7, the accelerating vortex soliton remains stable in the presence of a relatively strong contact self-attraction with $\beta_1 + \beta_2 = 10$ in Eq. (21), in spite of the well-known propensity of the cubic self-attraction to destabilize 2D vortex-ring solitons against the collapse and ring splitting [88]. Note also that the action of the self-attraction

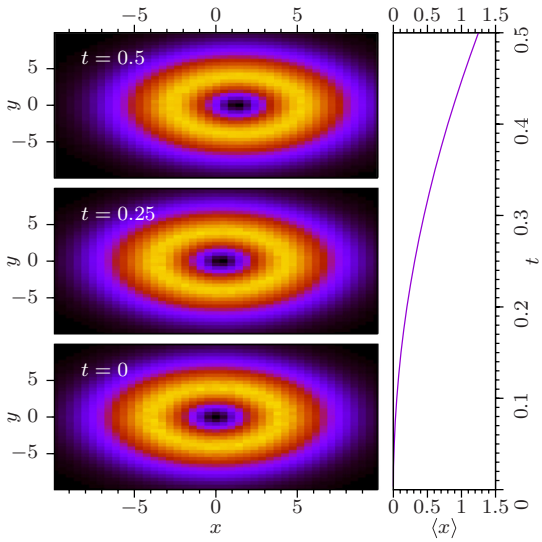

FIG. 6. Plot of $|\Phi_\downarrow|^2 = |\Phi_\uparrow|^2$ for a stable self-accelerating vortex soliton with $a_x = 10$, $a_y = 0$, $V_{x,y} = 0$, $\beta_{1,2} = 0$ [no contact interactions in Eq. (21)], and $\gamma = \pi$. The right panel shows the time evolution of coordinate x of the vortex center.

naturally leads to compression of the vortex ring. Finally, it is relevant to stress that the acceleration observed in Figs. 6 and 7 is much larger than in Figs. 3–5, because in the latter case it was induced by small random perturbations initially added to the 1D solitons, while in the situation displayed in Figs. 6 and 7 the acceleration was explicitly added to the input generating the 2D vortex solitons, as per Eq. (23).

B. The nonlocal optical system

The mechanism of the formation of the tailless self-accelerating solitons, elaborated above in terms of the two-component BEC coupled by the MW field, can be realized

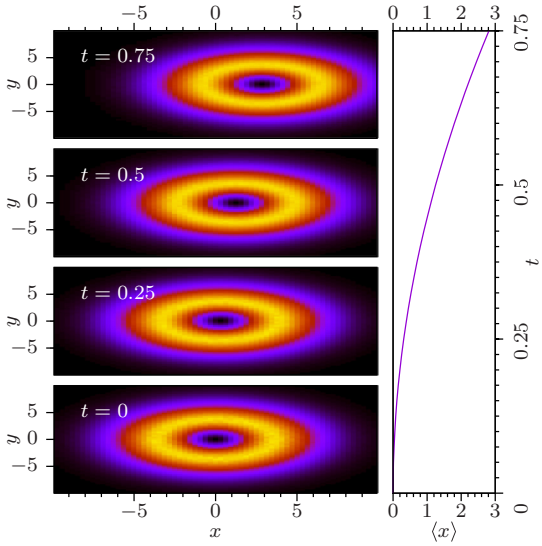

FIG. 7. Same as in Fig. 6, but in the presence of relatively strong contact self-attraction, represented by the coefficient $\beta_1 + \beta_2 = 10$ in Eq. (21).

as well in a nonlocal optical model with amplitude $E(x, y, z)$ of the electromagnetic wave and local perturbation $n(x, y, z)$ of the refractive index, which are governed by the coupled system of the paraxial propagation equation and an equation which determines how the index perturbation is created by the field distribution [89]:

$$iE_z + (1/2)(E_{xx} + E_{yy}) + nE = 0, \tag{25}$$

$$n - l^2(n_{xx} + n_{yy}) = |E|^2. \tag{26}$$

Here z is the propagation distance, x and y are transverse coordinates, and l is the correlation length of the nonlocality. Rescaling $E \equiv l\mathcal{E}$ and taking the limit of strong nonlocality $n/l \to 0$, Eqs. (25) and (26) are reduced to a form tantamount to Eqs. (21) and (22):

$$\begin{aligned} i\mathcal{E}_z + \tfrac{1}{2}(\mathcal{E}_{xx} + \mathcal{E}_{yy}) + n\mathcal{E} = 0, \\ n_{xx} + n_{yy} = -|\mathcal{E}|^2. \end{aligned} \tag{27}$$

The 1D reduction of the 2D system (27) is obviously possible too. Thus, stable 1D and 2D self-accelerating solitons may also be predicted in this optical setting.

V. CONCLUSION

The objective of this work was to investigate the dynamics of the binary BEC whose components, representing different hyperfine atomic states, are coupled by the magnetic component of the microwave field. In the general case, the spin-orbit coupling is included too. The effective interaction between the two components via the feedback of the atomic states on the MW field supports self-trapped modes (solitons), whose asymptotic form is the same as that of the Airy function, in the 1D case. In the presence of SOC, we have found stable 1D solitons of the regular (single-peak) and stripe types and solitons in the form of envelopes carried by plane waves. The most essential finding is the existence of stable self-accelerating solitons of the plane-wave type and their 2D counterparts, including vortex solitons. In contrast to the previously studied self-accelerating Airy waves [2], in the present system the solitons keep simple self-trapped shapes, without oscillatory tails attached to them, hence their integral norm is well defined and convergent, unlike the divergent norm of the exact Airy waves. The present system, being conservative, is also different from previously studied models which admit self-acceleration of localized modes in optical media featuring nonconservative effects, such as the sliding filtering, diffusion, ionization, and stimulated Raman scattering. The existence of the family of the self-accelerating solitons is demonstrated analytically, by reducing the two-component systems, in the 1D and 2D settings alike, to a single GPE, coupled to the Poisson equation for the potential of the MW field. These reduced systems admit the exact transformation to a reference frame moving with arbitrary acceleration, thus generating self-accelerating solitons from quiescent ones in the exact form. In the 2D geometry, the transformation generates 2D solitons which may move along curved trajectories, due to the interplay between the 2D velocity and acceleration. The self-acceleration mechanism persists if the contact nonlinearity is included. It can also be realized in strongly nonlocal optical media, with the 1D or 2D transverse geometry.

ACKNOWLEDGMENTS

G.D. acknowledges support from the National Science Foundation of China (Grants No. 11574085, No. 91536218 and No. 11834003), the 111 Project (No. B12024), the National Key Research and Development Program of China (Grant No. 2017YFA0304201), and the Innovation Program of Shanghai Municipal Education Commission. Z.L. acknowledges support from the National Science Foundation of China (Grant No. 11374125), the key projects of the Natural Science Foundation of China (Grant No. 11835011), and Youth Innovation Promotion Association of the Chinese Academy of Sciences (Grant No. 2013125). J.Q. acknowledges support from the National Science Foundation of China (Grant No. 11847059). The work of B.A.M. was supported in part by the joint program in physics between NSF and Binational (U.S.-Israel) Science Foundation through Project No. 2015616 and by the Israel Science Foundation through Grant No. 1286/17. B.A.M. appreciates the hospitality of the State Key Laboratory of Precision Spectroscopy at East China Normal University (Shanghai).

[1] M. V. Berry and N. L. Balazs, Am. J. Phys. **47**, 264 (1979).

[2] G. A. Siviloglou and D. N. Christodoulides, Opt. Lett. **32**, 979 (2007); G. A. Siviloglou, J. Broky, A. Dogariu, and D. N. Christodoulides, Phys. Rev. Lett. **99**, 213901 (2007); Opt. Lett. **33**, 207 (2008); R. El-Ganainy, K. G. Makris, M. A. Miri, D. N. Christodoulides, and Z. Chen, Phys. Rev. A **84**, 023842 (2011); P. Rose, F. Diebel, M. Boguslawski, and C. Denz, Appl. Phys. Lett. **102**, 101101 (2013); R. Driben, Y. Hu, Z. Chen, B. A. Malomed, and R. Morandotti, Opt. Lett. **38**, 2499 (2013); N. R. Bernier, L. D. Tóth, A. K. Feofanov, and T. J. Kippenberg, Phys. Rev. A **98**, 023841 (2018).

[3] A. Salandrino and D. N. Christodoulides, Opt. Lett. **35**, 2082 (2010); A. Minovich, A. E. Klein, N. Janunts, T. Pertsch, D. N. Neshev, and Y. S. Kivshar, Phys. Rev. Lett. **107**, 116802 (2011); L. Li, T. Li, S. M. Wang, C. Zhang, and S. N. Zhu, *ibid.* **107**, 126804 (2011); I. Epstein and A. Arie, *ibid.* **112**, 023903 (2014); A. Libster-Hershko, I. Epstein, and A. Arie, *ibid.* **113**, 123902 (2014); A. E. Minovich, A. E. Klein, D. N. Neshev, T. Pertsch, Y. S. Kivshar, and D. N. Christodoulides, Laser Photon. Rev. **8**, 221 (2014).

[4] P. Zhang, T. Li, J. Zhu, X. Zhu, S. Yang, Y. Wang, X. Yin, and X. Zhang, Nat. Commun. **5**, 4316 (2014); U. Bar-Ziv, A. Postan, and M. Segev, Phys. Rev. B **92**, 100301(R) (2015).

[5] M. Clerici, Y. Hu, P. Lassonde, C. Milian, A. Couairon, D. N. Christodoulides, Z. Chen, L. Razzari, F. Vidal, F. Legare, D. Faccio, and R. Morandotti, Sci. Adv. **1**, e1400111 (2015).

[6] S. Fu, Y. Tsur, J. Zhou, L. Shemer, and A. Arie, Phys. Rev. Lett. **115**, 034501 (2015).

[7] P. Polynkin, M. Kolesik, J. V. Moloney, G. A. Siviloglou, and D. N. Christodoulides, Science **324**, 229 (2009).

[8] Y. Liang, Y. Hu, D. Song, C. Lou, X. Zhang, Z. Chen, and J. Xu, Opt. Lett. **40**, 5686 (2015).

[9] S. Jia, J. C. Vaughan, and X. Zhuang, Nat. Photon. **8**, 302 (2014).

[10] P. Polynkin, M. Kolesik, and J. Moloney, Phys. Rev. Lett. **103**, 123902 (2009).

[11] Z. Zheng, B. F. Zhang, H. Chen, J. Ding, and H. T. Wang, Appl. Opt. **50**, 43 (2011).

[12] R. Cao, Y. Yang, J. Wang, J. Bu, M. Wang, and X. C. Yuan, Appl. Phys. Lett. **99**, 261106 (2011); Y. Zhang, H. Zhong, M. R. Belić, and Y. Zhang, Appl. Sci. **7**, 341 (2017).

[13] J. Baumgartl, M. Mazilu, and K. Dholakia, Nat. Photon. **2**, 675 (2008).

[14] P. Zhang, J. Prakash, Z. Zhang, M. S. Mills, N. K. Efremidis, D. N. Christodoulides, and Z. Chen, Opt. Lett. **36**, 2883 (2011).

[15] R. Schley, I. Kaminer, E. Greenfield, R. Bekenstein, Y. Lumer, and M. Segev, Nat. Commun. **5**, 5189 (2014).

[16] T. Vettenburg, H. I. Dalgarno, J. Nylk, C. Coll-Lladó, D. E. Ferrier, T. Čižmár, F. J. Gunn-Moore, and K. Dholakia, Nat. Methods **11**, 541 (2014).

[17] D. Abdollahpour, S. Suntsov, D. G. Papazoglou, and S. Tzortzakis, Phys. Rev. Lett. **105**, 253901 (2010).

[18] A. Chong, W. H. Renninger, D. N. Christodoulides, and F. W. Wise, Nat. Photon. **4**, 103 (2010).

[19] C. Ament, P. Polynkin, and J. V. Moloney, Phys. Rev. Lett. **107**, 243901 (2011).

[20] K. Y. Kim, C. Y. Hwang, and B. Lee, Opt. Express **19**, 2286 (2011).

[21] Y. Gu and G. Gbur, Opt. Lett. **35**, 3456 (2010).

[22] J. Baumgartl, T. Čižmár, M. Mazilu, V. C. Chan, A. E. Carruthers, B. A. Capron, W. McNeely, E. M. Wright, and K. Dholakia, Opt. Exp. **18**, 17130 (2010).

[23] J. Zhao, I. D. Chremmos, D. Song, D. N. Christodoulides, N. K. Efremidis, and Z. Chen, Sci. Rep. **5**, 12086 (2015).

[24] N. Voloch-Bloch, Y. Lereah, Y. Lilach, A. Gover, and A. Arie, Nature (London) **494**, 331 (2013).

[25] I. Kaminer, J. Nemirovsky, M. Rechtsman, R. Bekenstein, and M. Segev, Nat. Phys. **11**, 261 (2015).

[26] N. K. Efremidis, V. Paltoglou, and W. von Klitzing, Phys. Rev. A **87**, 043637 (2013).

[27] C. Yuce, Mod. Phys. Lett. B **29**, 1550171 (2015).

[28] P. Panagiotopoulos, D. Abdollahpour, A. Lotti, A. Couairon, D. Faccio, D. G. Papazoglou, and S. Tzortzakis, Phys. Rev. A **86**, 013842 (2012).

[29] T. Ellenbogen, N. Voloch-Bloch, A. Ganany-Padowicz, and A. Arie, Nat. Photon. **3**, 395 (2009).

[30] S. Jia, J. Lee, J. W. Fleischer, G. A. Siviloglou, and D. N. Christodoulides, Phys. Rev. Lett. **104**, 253904 (2010).

[31] M. Shen, J. Gao, and L. Ge, Sci. Rep. **5**, 9814 (2014).

[32] Y. Hu, S. Huang, P. Zhang, C. Lou, J. Xu, and Z. Chen, Opt. Lett. **35**, 3952 (2010).

[33] I. Kaminer, M. Segev, and D. N. Christodoulides, Phys. Rev. Lett. **106**, 213903 (2011).

[34] A. Lotti, D. Faccio, A. Couairon, D. G. Papazoglou, P. Panagiotopoulos, D. Abdollahpour, and S. Tzortzakis, Phys. Rev. A **84**, 021807 (2011).

[35] Y. Fattal, A. Rudnick, and D. M. Marom, Opt. Express **19**, 17298 (2011).

[36] A. Rudnick and D. M. Marom, Opt. Express **19**, 25570 (2011).

[37] P. Zhang, Y. Hu, D. Cannan, A. Salandrino, T. Li, R. Morandotti, X. Zhang, and Z. Chen, Opt. Lett. **37**, 2820 (2012).

[38] I. Kaminer, J. Nemirovsky, and M. Segev, Opt. Express **20**, 18827 (2012).

[39] I. Dolev, I. Kaminer, A. Shapira, M. Segev, and A. Arie, Phys. Rev. Lett. **108**, 113903 (2012).

[40] R. Driben, V. V. Konotop, and T. Meier, Opt. Lett. **39**, 5523 (2014).

[41] I. M. Allayarov and E. N. Tsoy, Phys. Rev. A **90**, 023852 (2014).

[42] T. Mayteevarunyoo and B. A. Malomed, Opt. Lett. **40**, 4947 (2015); **41**, 2919 (2016); J. Opt. **19**, 085501 (2017).

[43] S. Batz and U. Peschel, Phys. Rev. Lett. **110**, 193901 (2013); H. Sakaguchi and B. A. Malomed, Phys. Rev. E (to be published).

[44] M. Wimmer, A. Regensburger, C. Bersch, M.-A. Miri, S. Batz, G. Onishchukov, D. N. Christodoulides, and U. Peschel, Nat. Phys. **9**, 780 (2013).

[45] L. F. Mollenauer, J. P. Gordon, and S. G. Evangelides, Opt. Lett. **17**, 1575 (1992); P. V. Mamyshev and L. F. Mollenauer, *ibid.* **19**, 2083 (1994); S. Burtsev and D. J. Kaup, J. Opt. Soc. Am. B **14**, 627 (1997); B. A. Malomed and R. S. Tasgal, *ibid.* **15**, 162 (1998); M. Facão and D. F. Parker, Phys. Rev. E **71**, 066611 (2005).

[46] E. V. Vanin, A. I. Korytin, A. M. Sergeev, D. Anderson, M. Lisak, and L. Vázquez, Phys. Rev. A **49**, 2806 (1994); M. Facão, M. I. Carvalho, and P. Almeida, *ibid.* **87**, 063803 (2013); M. Facão and M. I. Carvalho, Appl. Phys. B **116**, 353 (2014).

[47] M. I. Carvalho, S. R. Singh, and D. N. Christodoulides, Opt. Commun. **120**, 311 (1995); M. Facão and D. F. Parker, Phys. Rev. E **68**, 016610 (2003).

[48] F. M. Mitschke and L. F. Mollenauer, Opt. Lett. **11**, 659 (1986); J. P. Gordon, *ibid.* **11**, 662 (1986); K. J. Blow and D. Wood, IEEE J. Quantum Electron. **25**, 2665 (1989); M. Facão, M. I. Carvalho, and D. F. Parker, Phys. Rev. E **81**, 046604 (2010).

[49] J. Qin, G. Dong, and B. A. Malomed, Phys. Rev. Lett. **115**, 023901 (2015).

[50] J. Qin, G. Dong, and B. A. Malomed, Phys. Rev. A **94**, 053611 (2016).

[51] M. Kauranen and A. V. Zayats, Nat. Photon. **6**, 737 (2012); I. Carusotto and C. Ciuti, Rev. Mod. Phys. **85**, 299 (2013); C. Schneider, K. Winkler, M. D. Fraser, M. Kamp, Y. Yamamoto, E. A. Ostrovskaya, and S. Höfling, Rep. Prog. Phys. **80**, 016503 (2017).

[52] Y.-J. Lin, K. Jiménez-García, and I. B. Spielman, Nature (London) **471**, 83 (2011); P. Wang, Z.-Q. Yu, Z. Fu, J. Miao, L. Huang, S. Chai, H. Zhai, and J. Zhang, Phys. Rev. Lett. **109**, 095301 (2012); L. W. Cheuk, A. T. Sommer, Z. Hadzibabic, T. Yefsah, W. S. Bakr, and M. W. Zwierlein, *ibid.* **109**, 095302 (2012).

[53] Y.-J. Lin, R. L. Compton, A. R. Perry, W. D. Phillips, J. V. Porto, and I. B. Spielman, Phys. Rev. Lett. **102**, 130401 (2009); Y.-J. Lin, R. L. Compton, K. Jimenez-Garcia, J. V. Porto, and I. B. Spielman, Nature (London) **462**, 628 (2009); Y.-J. Lin, R. L. Compton, K. Jimenez-Garcia, W. D. Phillips, J. V. Porto, and I. B. Spielman, Nat. Phys. **7**, 531 (2011); J. Dalibard, F. Gerbier, G. Juzeliūnas, and P. Öhberg, Rev. Mod. Phys. **83**, 1523 (2011).

[54] J.-Y. Zhang, S.-C. Ji, Z. Chen, L. Zhang, Z.-D. Du, B. Yan, G.-S. Pan, B. Zhao, Y.-J. Deng, H. Zhai, S. Chen, and J.-W. Pan, Phys. Rev. Lett. **109**, 115301 (2012).

[55] A. J. Olson, S.-J. Wang, R. J. Niffenegger, C.-H. Li, C. H. Greene, and Y. P. Chen, Phys. Rev. A **90**, 013616 (2014).

[56] M. Aidelsburger, M. Atala, M. Lohse, J. T. Barreiro, B. Paredes, and I. Bloch, Phys. Rev. Lett. **111**, 185301 (2013).

[57] H. Miyake, G. A. Siviloglou, C. J. Kennedy, W. C. Burton, and W. Ketterle, Phys. Rev. Lett. **111**, 185302 (2013).

[58] C. Qu, C. Hamner, M. Gong, C. Zhang, and P. Engels, Phys. Rev. A **88**, 021604 (2013).

[59] G. Jotzu, M. Messer, R. Desbuquois, M. Lebrat, T. Uehlinger, D. Greif, and T. Esslinger, Nature (London) **515**, 237 (2014).

[60] C. V. Parker, L.-C. Ha, and C. Chin, Nat. Phys. **9**, 769 (2013).

[61] J. Struck, M. Weinberg, C. Ölschläger, P. Windpassinger, J. Simonet, K. Sengstock, R. Höppner, P. Hauke, A. Eckardt, M. Lewenstein, and L. Mathey, Nat. Phys. **9**, 738 (2013).

[62] B. K. Stuhl, H.-I. Lu, L. M. Aycock, D. Genkina, and I. B. Spielman, Science **349**, 1514 (2015).

[63] M. Mancini, G. Pagano, G. Cappellini, L. Livi, M. Rider, J. Catani, C. Sias, P. Zoller, M. Inguscio, M. Dalmonte, and L. Fallani, Science **349**, 1510 (2015).

[64] N. Q. Burdick, Y. Tang, and B. L. Lev, Phys. Rev. X **6**, 031022 (2016).

[65] B. Song, C. He, S. Zhang, E. Hajiyev, W. Huang, X.-J. Liu, and G.-B. Jo, Phys. Rev. A **94**, 061604 (2016).

[66] S. Kolkowitz, S. L. Bromley, T. Bothwell, M. L. Wall, G. E. Marti, A. P. Koller, X. Zhang, A. M. Rey, and J. Ye, Nature (London) **542**, 66 (2017).

[67] L. F. Livi, G. Cappellini, M. Diem, L. Franchi, C. Clivati, M. Frittelli, F. Levi, D. Calonico, J. Catani, M. Inguscio, and L. Fallani, Phys. Rev. Lett. **117**, 220401 (2016).

[68] L. Huang, Z. Meng, P. Wang, P. Peng, S.-L. Zhang, L. Chen, D. Li, Q. Zhou, and J. Zhang, Nat. Phys. **12**, 540 (2016).

[69] Z. Wu, L. Zhang, W. Sun, X.-T. Xu, B.-Z. Wang, S.-C. Ji, Y. Deng, S. Chen, X.-J. Liu, and J.-W. Pan, Science **354**, 83 (2016).

[70] C. Wang, C. Gao, C.-M. Jian, and H. Zhai, Phys. Rev. Lett. **105**, 160403 (2010).

[71] Y. Li, L. P. Pitaevskii, and S. Stringari, Phys. Rev. Lett. **108**, 225301 (2012).

[72] J.-R. Li, J. Lee, W. Huang, S. Burchesky, B. Shteynas, F. C. Top, A. O. Jamison, and W. Ketterle, Nature (London) **543**, 91 (2017).

[73] T. L. Ho and S. Zhang, Phys. Rev. Lett. **107**, 150403 (2011).

[74] W. Han, G. Juzeliūnas, W. Zhang, and W. M. Liu, Phys. Rev. A **91**, 013607 (2015).

[75] Y. Li, G. I. Martone, L. P. Pitaevskii, and S. Stringari, Phys. Rev. Lett. **110**, 235302 (2013); D. A. Zezyulin, R. Driben, V. V. Konotop, and B. A. Malomed, Phys. Rev. A **88**, 013607 (2013).

[76] O. Fialko, J. Brand, and U. Zülicke, Phys. Rev. A **85**, 051605 (2012); V. Achilleos, D. J. Frantzeskakis, P. G. Kevrekidis, and D. E. Pelinovsky, Phys. Rev. Lett. **110**, 264101 (2013); Y. V. Kartashov, V. V. Konotop, and F. K. Abdullaev, *ibid.* **111**, 060402 (2013); L. Salasnich and B. A. Malomed, Phys. Rev. A **87**, 063625 (2013); V. E. Lobanov, Y. V. Kartashov, and V. V. Konotop, Phys. Rev. Lett. **112**, 180403 (2014); P. Beličev, G. Gligorić, J. Petrović, A. Maluckov, L. Hadzievski, and B. A. Malomed, J. Phys. B **48**, 065301 (2015); L. Wen, Q. Sun, Y. Chen, D.-S. Wang, J. Hu, H. Chen, W.-M. Liu, G. Juzeliūnas, B. A. Malomed, and A.-C. Ji, Phys. Rev. A **94**, 061602 (2016).

[77] Y. Xu, Y. Zhang, and B. Wu, Phys. Rev. A **87**, 013614 (2013).

[78] H. Sakaguchi, B. Li, and B. A. Malomed, Phys. Rev. E **89**, 032920 (2014).

[79] Y. Xu, Y. Zhang, and C. Zhang, Phys. Rev. A **92**, 013633 (2015).

[80] X. Jiang, Z. Fan, Z. Chen, W. Pang, Y. Li, and B. A. Malomed, Phys. Rev. A **93**, 023633 (2016); H. Sakaguchi, E. Y. Sherman, and B. A. Malomed, Phys. Rev. E **94**, 032202 (2016); H. Sakaguchi, B. Li, E. Ya. Sherman, and B. A. Malomed, Rom. Rep. Phys. **70**, 502 (2018); B. Liao, S. Li, C. Huang, Z. Luo, W. Pang, H. Tan, B. A. Malomed, and Y. Li, Phys. Rev. A **96**, 043613 (2017); S. Gautam and S. K. Adhikari, *ibid.* **95**, 013608 (2017); G. Chen, Y. Liu, and H. Wang, Commun. Nonlinear Sci. Numer. Simul. **48**, 318 (2017); Y. Zhang, M. E. Mossman, T. Busch, P. Engels, and C. Zhang, Front. Phys. **11**, 118103 (2016); Y. Li, Y. Liu, Z. Fan, W. Pang, S. Fu, and B. A. Malomed, Phys. Rev. A **95**, 063613 (2017); H. Sakaguchi and B. A. Malomed, *ibid.* **96**, 043620 (2017); Y. Li, Z. Luo, Y. Liu, Z. Chen, C. Huang, S. Fu, H. Tan, and B. A. Malomed, New J. Phys. **19**, 113043 (2017).

[81] Y.-C. Zhang, Z.-W. Zhou, B. A. Malomed, and H. Pu, Phys. Rev. Lett. **115**, 253902 (2015).

[82] B. A. Malomed, Europhys. Lett. **122**, 36001 (2018).

[83] K. V. Krutitsky, K. P. Marzlin, and J. Audretsch, Laser Phys. **11**, 449 (2001); J. Zhu, G. Dong, M. N. Shneider, and W. Zhang, Phys. Rev. Lett. **106**, 210403 (2011); G. Dong, J. Zhu, W. Zhang, and B. A. Malomed, *ibid.* **110**, 250401 (2013).

[84] K. M. van der Stam, E. D. van Ooijen, R. Meppelink, J. M. Vogels, and P. van der Straten, Rev. Sci. Instrum. **78**, 013102 (2007); H. Imai, T. Akatsuka, T. Ode, and A. Morinaga, Phys. Rev. A **85**, 013633 (2012).

[85] H. Zhai, Rep. Prog. Phys. **78**, 026001 (2015).

[86] L. Gagnon and P. A. Bélanger, Opt. Lett. **15**, 466 (1990).

[87] D. F. Parker, C. Sophocleous, and C. Radha, J. Phys. A: Math. Gen. **35**, 1283 (2002).

[88] B. A. Malomed, D. Mihalache, F. Wise, and L. Torner, J. Opt. B **7**, R53 (2005); B. A. Malomed, Eur. Phys. J. Spec. Top. **225**, 2507 (2016).

[89] A. Minovich, D. N. Neshev, A. Dreischuh, W. Królikowski, and Y. S. Kivshar, Opt. Lett. **32**, 1599 (2007).